An Order of Magnitude Improved Limit on the Electron Electric Dipole Moment

ACME Collaboration: Daniel G. Ang,[1] Cole Meisenhelder,[1] Xing Wu,[1,2] Vitaly Andreev,[1] Piroz Bahar,[1] David DeMille[2] (PI), John M. Doyle[1] (PI), Gerald Gabrielse[3] (PI), Jonathan Haefner,[1] Zhen Han,[1] Nicholas R. Hutzler,[4] Zack D. Lasner,[2] Brendon R. O'Leary,[2] Cristian D. Panda,[1] Adam D. West,[2] Elizabeth P. West[1]

Affiliation: [1]Harvard University, [2]Yale University, [3]Northwestern University, [4]California Institute of Technology

Motivation & Theory

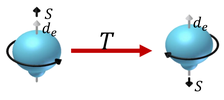

Permanent EDMs violate T-symmetry. Many theories beyond the Standard Model predict T violation and EDMs at current experimental precision.

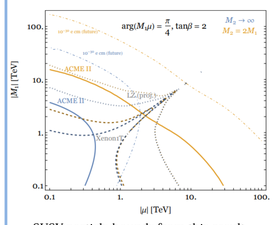

SUSY particle bounds from this result. Fig. from Matt Reece (unpublished). ACME III proj. ($\sim 10^{-30}$ e ·cm) dashed.

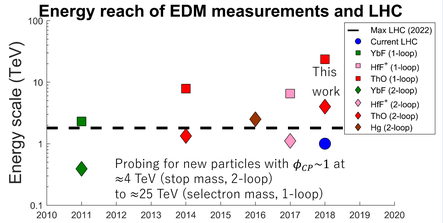

Key EDM results since 2010. Two-loop sensitivity from Nakai & Reece (2017).

One-loop sensitivity from Feng (2013). LHC scale gives stop mass sensitivity.

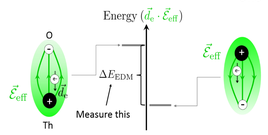

$$\delta d_e = \frac{\hbar}{2C\tau\mathcal{E}_{\rm eff}\sqrt{\dot{n}T}}$$

Effective electric field $\mathcal{E}_{\rm eff}$: ~ 80 GV/cm
Precession time τ : ~ 1 ms
Measurement contrast $\mathcal{C}$: ~ 0.95
(Detected) molecule flux $\dot{n}$:
ACME I: $\sim 3\times 10^4\ s^{-1}$
ACME II: $\sim 1\times 10^7\ s^{-1}$
ACME I result $d_e = (-2.2 \pm 4.8)\times 10^{-29}$ e · cm
$\Rightarrow |d_e| < 9.3\times 10^{-29}$ e · cm
ACME II result $d_e = (4.3 \pm 4.0)\times 10^{-30}$ e · cm
$\Rightarrow |d_e| < 1.1\times 10^{-29}$ e · cm

1. Buffer gas beam source

ThO in the gas phase is produced through **pulsed ablation of a ceramic ThO_2 target** with an Nd:YAG laser. Ablation is performed at 50 Hz in a cryogenic buffer gas cell. The ThO molecules thermalize with and are entrained in the flow of the neon buffer gas. The molecular beam is cooled to 4 K. Each pulse produces a flux of ~10^{11} molecules per steradian in the electro-vibrational ground state.

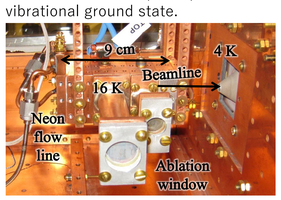

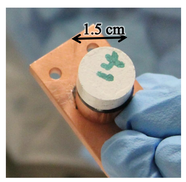

Ceramic ThO_2 ablation target

2. Rotational Cooling

The molecules in the X state are primarily distributed in the lowest four rotational states after leaving the cell. Optical pumping on the $X-C$ transition transfers population from the $J=0,1,2$ levels to the $J=0$ level, increasing usable molecule flux by a factor of ~2.7.

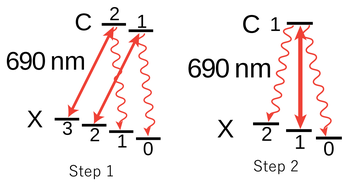

3. State Preparation

The EDM measurement is performed in the metastable H state. STIRAP **coherently transfers population** through an intermediate short-lived state to the spin-aligned state that represents the beginning of the EDM measurement. This transfer occurs with an efficiency of ~75%.

STIRAP Level Structure

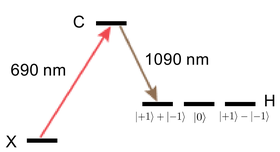

Cleanup Level Structure

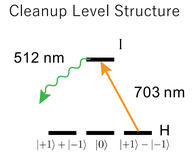

A separate 703 nm cleanup laser reprojects the spin-aligned state prepared by the STIRAP lasers onto a coherent superposition of $M=+1, M=-1$ states, suppressing possible EDM-like phases caused by the STIRAP beams.

ACME II Apparatus

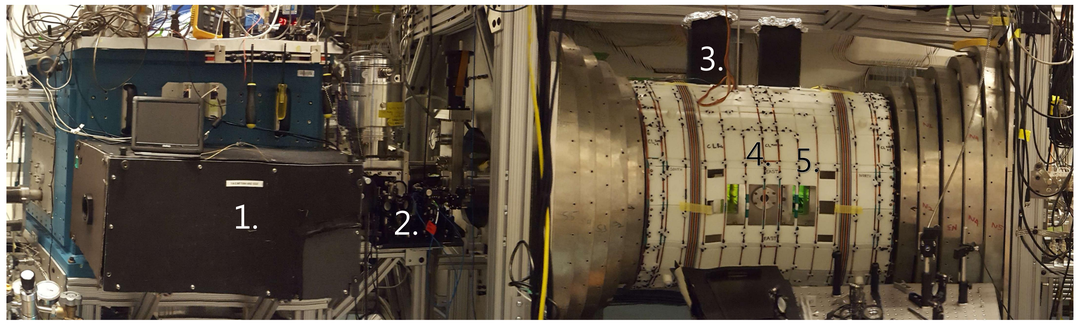

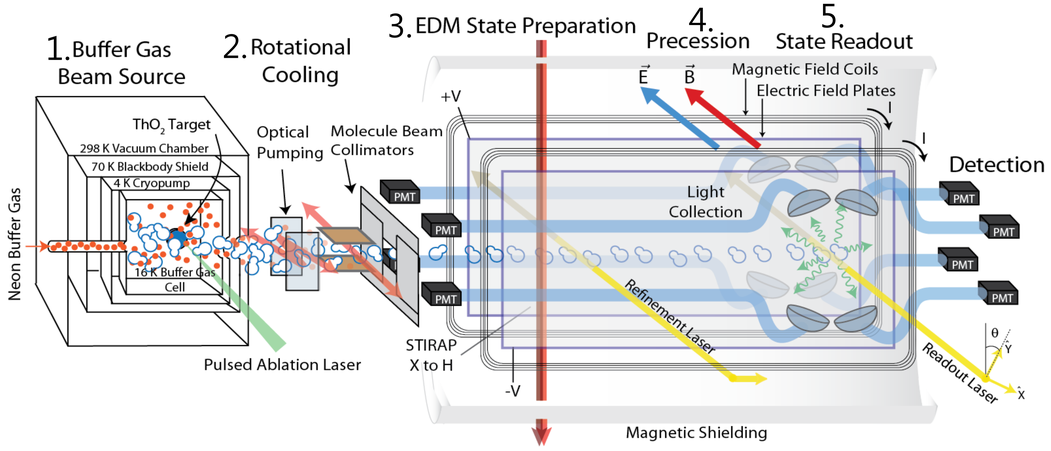

4. State Precession

The molecules in the prepared state **precess and acquire phase** as they fly through the electric and magnetic fields of the interaction region.

$$\frac{1}{\sqrt{2}}(|-1\rangle+|+1\rangle) \longrightarrow \frac{1}{\sqrt{2}}(e^{i\phi}|-1\rangle+e^{-i\phi}|+1\rangle)$$

$$\frac{\phi}{\tau} = -(\tilde{\mathcal{B}} g_1 \mu_B \mathcal{B}_z + \tilde{N}\tilde{\mathcal{E}} d_e \mathcal{E}_{\rm eff})$$

5. State Readout

At the end of the interaction region, the final state is **projected to a pair of orthogonal basis vectors** by subjecting the molecules to a 703 nm probe laser (on the H-I transition) with linear polarization rapidly switched (200 kHz) between x and y.

We **collect the 512 nm fluorescence** using PMTs as the molecules in the short-lived I-state decay back to the ground state.

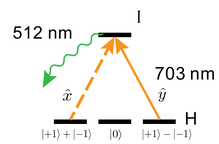

Data Acquisition Structure

The spin precession is performed with different configurations of parameters that switch the sign of the different terms that contribute to the phase.

This enables us to **extract the EDM contribution to the phase** by performing "**parity sums**" of the different phases taken under different conditions, and also diagnose and suppress known systematic errors.

By performing the experiment with different values of $\tilde{N}$, $\tilde{E}$, $\tilde{B}$ we can extract **the EDM channel $\phi^{\tilde{N}\tilde{E}}$**, the component of the phase which is odd under reversal of $\tilde{N}$ and $\tilde{E}$.

This measurement scheme results in robust suppression of systematic effects: any imperfections in the system would have to be correlated with $\tilde{N}$ and $\tilde{E}$ to become a source of systematic error.

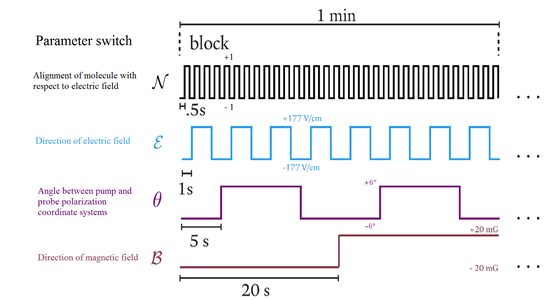

Degeneracy of States: 4

$$\omega(\tilde{N},\tilde{E},\tilde{B}) = \tilde{N}\omega^{\tilde{N}} + \tilde{E}\omega^{\tilde{E}} + \tilde{B}\omega^{\tilde{B}} + \tilde{N}\tilde{E}\omega^{\tilde{N}\tilde{E}} + \tilde{N}\tilde{B}\omega^{\tilde{N}\tilde{B}} + \tilde{E}\tilde{B}\omega^{\tilde{E}\tilde{B}} + \tilde{N}\tilde{E}\tilde{B}\omega^{\tilde{N}\tilde{E}\tilde{B}}$$
$$\tilde{N},\tilde{E},\tilde{B} \in \{+1,-1\}$$

EDM frequency

Systematic Search & Characterization

Parameter	Uncertainty ($10^{-30} e \cdot cm$)	
Non-reversing Electric Field, $\mathcal{E}^{nr}$	1.18	These parameters showed shifts in the EDM channel
$\tilde{N}\tilde{E}$ and $\tilde{N}\tilde{E}\tilde{B}$ correlated contrast variations, $\lvert\mathcal{C}\rvert^{\tilde{N}\tilde{\mathcal{E}}}$, $\lvert\mathcal{C}\rvert^{\tilde{N}\tilde{\mathcal{E}}\tilde{\mathcal{B}}}$	1.05	
Magnetic field gradients, $\frac{\partial\mathcal{B}_z}{\partial z}$, $\frac{\partial\mathcal{B}_z}{\partial y}$	0.50	
STIRAP $\tilde{N}\tilde{E}$ correlated phase $\omega_{ST}^{\tilde{N}\tilde{E}}$	0.008	
$\tilde{E}$ correlated phases, $\phi^{\tilde{E}}$	0.008	
⋮	⋮	40 total parameters were varied during systematic checks
⋮	⋮	
Total Systematic	2.61	

We varied 40 different experiment parameters in the search for systematic errors. These include magnetic fields, electric fields, laser powers, laser detunings, laser pointing, laser polarization, molecular beam clipping, experiment timing, and analysis.

Where possible, we intentionally exaggerate the parameter and assume ω depends linearly on the parameter P. The systematic error under ordinary conditions ($P=\bar{P}$) is given as

$$\omega_{\rm P}^{\tilde{N}\tilde{E}} = \left(\partial\omega^{\tilde{N}\tilde{E}}/\partial P\right)\bar{P}$$

The final contribution to the systematic uncertainty is computed from the linear error propagation of the two variables $\bar{P}$ and $\partial\omega^{\tilde{N}\tilde{E}}/\partial P$.

Proposed ACME III Improvements

Molecular Lens

Due to molecular beam divergence, only 0.05% of molecules reach the detection region. An electrostatic lens can significantly increase molecular flux by focusing molecules in the electrically-sensitive Q (J=2) state into the measurement region.

Increased Precession Time

Recent measurements determined that the H state lifetime of ThO is 4-6 ms. This is 4-6 times longer than the ACME II precession time. Combined with the molecular lens, increasing the precession region length by roughly 1 m will significantly increase measurement sensitivity.

Optical Cycling

Only ~5% of fluorescence from the spin-precessed molecules was detected, due to losses from collection optics and quantum efficiency. Photon cycling on a relatively closed transition (I-X, 91%) will increase the number of photons emitted per molecule. Combined with planned improvements to collection optics and detector upgrades, this might result in at least an order of magnitude increase in signal.

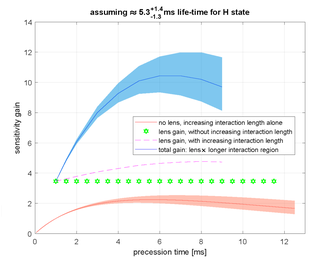

Plot of sensitivity gain versus precession time with and without the molecular lens.

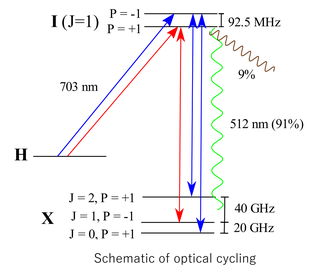

Schematic of optical cycling

Outlook

We are currently pursuing upgrades to the ACME apparatus with the goal of at least an order of magnitude improvement in measurement sensitivity.

Upgrade	Parameter Improved	Sensitivity Increase
Noise Suppresion	Timing Jitter	1.7
Molecular Lens	Mol. Beam Divergence	4.6
Optical Cycling	Detection Efficiency	2.9
Longer Interaction Region	Increased Precession Time	2.3
Total		52

References

ACME II result: V Andreev et al., *Nature* **562**, 355-360 (2018)
ACME I result: J Baron et al., *Science* **343**, 269-272 (2014)
ACME I detailed report: J Baron et al., *New J. Phys.***19** (2017)
$E_{\rm eff}$ Calculations: L. V. Skripnikov et al., *J. Chem. Phys.* **142** 024301 (2015), T. Fleig et al., *J. Mol. Spec.* **300** p. 16-21 (2014)
EDM & SUSY: J. Feng, Annu. Rev. Nucl. Part. Sci., **63**:35,1-82 (2013), Y. Nakai, et al., *J. High Energy Phys.* **2017**:31 (2017)
Interpreting the Electron EDM Constraint: C. Cesarotti et al., *arXiv* (2018)

More information: www.electronedm.info